Observation of dd excitations in NiO and NiCl_{2} using K-edge resonant inelastic x-ray scattering

Michel van Veenendaal, Xiaosong Liu, Matthew H. Carpenter, and Stephen P. Cramer

Phys. Rev. B **83**, 045101 — Published 10 January 2011

DOI: 10.1103/PhysRevB.83.045101

Observation of dd Excitations via $4p$-$3d$ Coulomb scattering in K-edge Resonant Inelastic Scattering in NiO and $NiCl_2$

Michel van Veenendaal[1,2], Xiaosong Liu[3], Matthew H. Carpenter[4], and Stephen P. Cramer[3,4]
[1]*Department of Physics, Northern Illinois University, De Kalb, IL 60115*
[2]*Advanced Photon Source, Argonne National Laboratory, 9700 South Cass Avenue, Argonne, IL 60439*
[3]*Physical Biosciences Division, Lawrence Berkeley National Laboratory, 1 Cyclotron Road, Berkeley, CA 94720*
[4]*Department of Applied Science, University of California, Davis, CA 95616*

The presence of dd excitations in K-edge resonant inelastic X-ray scattering in the $1s \rightarrow 4p$ region of transition-metal compounds and their excitation mechanism is established through measurements on NiO and $NiCl_2$. It is demonstrated that the valence excitations are due to the interaction between the excited $4p$ electron and the $3d$ valence electrons. A detailed analytical framework for interpreting these excitations in transition-metal compounds is presented demonstrating a strong angular dependence for different dd excitations.

PACS numbers: 78.70.Ck, 61.05.cc, 71.27.+a

I. INTRODUCTION

The study of complex materials under real conditions is often hampered by the lack of proper characterization tools that are both chemical and bulk selective. In optical spectroscopy, one is unable to distinguish excitations from different elements and, for transition-metal compounds, dd excitations are only allowed due to the simulaneous excitation of magnons or phonons. Resonant inelastic X-ray scattering (RIXS)[1], on the other hand, employs the excitation of an electron from a deeplying core level of a particular element into the valence shell through the absorption of an X-ray photon with energy $\hbar\omega$. One subsequently detects the energy $\hbar\omega'$ of the X-rays resulting from the radiative decay of the core hole. Local dd transitions[1], spin-flips[2], and single-magnon excitations[3] have been observed in the soft X-ray region at the transition-metal L- and M- edges. However, low-energy X-rays do not have sufficient penetration depth to study, for example, the electronic structure in technologically-relevant materials, such as transition-metal molecular compounds in solution. The use of hard X-rays allows the chemically-selective measurement of valence excitations under ambient conditions. For example, for nickel compounds, the focus of this paper, Ni is at the active site of several environmentally critical enzymes[8]. These include enzymes for H_2 production - [NiFe] hydrogenase[9], CH_4 production - methyl-coenzyme M reductase[10], and CO-CO_2 metabolism - CO dehydrogenase[11]. Given the multitude of controversies about the catalytic mechanisms of these enzymes, a new experimental probe of the electronic structure of nickel and other transition-metal compounds would have immediate application in this field.

At the K-edge, in the dipolar $1s \rightarrow 4p$ region, the focus of RIXS has been primarily on charge-transfer excitations with an energy of 2-6 eV[4]. These are generally considered to be a result of shake-up processes due to the strong Coulomb interaction with the $1s$ core-hole. Low-energy excitations (< 2 eV) in the hard X-ray region are more difficult to observe, but will become more easily accessible due to the rapidly-increasing advances in RIXS technology[5–7]. It has been shown that the $1s$ core-hole potential can possibly create bimagnon excitations[6]. In the weak pre-edge feature which is due to $1s \rightarrow 3d$ transitions, dd excitations can be observed since angular momentum is transferred via the polarization of the X-rays[5]. However, they are not expected at the main edge ($1s \rightarrow 4p$ transitions), since the $1s$ core-hole potential cannot transfer angular momentum to the valence shell. Despite of that, low-energy excitations are still observed at these absorption energies[7]. In the absence of a clear understanding of the excitation mechanism, a definite assignment of low-energy excitations in the dipolar region ($1s \rightarrow 4p$) remains difficult[6,7].

We demonstrate the presence of low-energy excitations in NiO and $NiCl_2$ in the $1s \rightarrow 4p$ excitation region. Since these materials are well studied, we can unequivocally ascribe the excitations to local dd transitions. We show that these excitations are a result of the $3d$-$4p$ Coulomb interaction. This mechanism leads to a clear angular dependence, which allows distinction from other low-energy excitations, such as, e.g. bimagnons[6]. This work opens the door to the study of active sites using hard X-rays.

II. EXPERIMENT

The experiments were performed at the MERIX undulator beamline of Sector 30 at the Advanced Photon Source, Argonne National Laboratory. Two monochromators are installed on the beamline. The first one is a water-cooled two-crystal diamond [111] monochromator with a measured bandwidth of 400 meV near the Ni K-edge. The second one is a 4-crystal backscatter monochromator with 70 meV resolution. The surface of the sample is aligned along 45° from the direction of beam incidence. The scattering angle is 90°. The fluorescence emission is detected with a near-backscatter spherically-bent diced-crystal spectrometer. The crys-

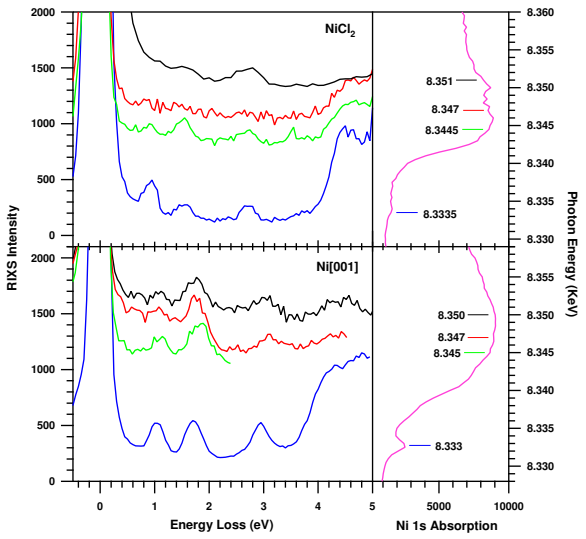

FIG. 1: Ni K-edge RIXS of NiO[001] and $NiCl_2$. The X-ray absorption is shown in the right panel. RIXS spectra for different excitation energy are shown in the left panel.

tal analyzer has a 1 m radius of curvature and 1 mm^2 segments (pixels), and is immersed in a He-atmosphere chamber to minimize scattering and absorption. A position-sensitive Si strip detector with 50-micron strips records the dispersed X-rays from the analyzer. The sample-analyzer-detector geometry is arranged on a Rowland circle, with the sample and analyzer in fixed positions and the detector movable about the circle. Two crystal analyzers were used: [642] Ge (resolution of 180 meV), and [01-10] $LiNbO_3$ (resolution of 140 meV) for energies above 8.342 keV.

The RIXS spectra are shown in Fig. 1 at different excitation energies for a single crsytal NiO[001] and polycrystalline $NiCl_2$. In the pre-edge region, quadrupolar transitions from the $1s$ into the $3d$ shell are observed. The dd transitions can be explained within an atomic multiplet framework[5]. In octahedral symmetry,[12] the ground state for Ni^{2+} is $\underline{d}^2_{e_g\uparrow}$ ($^3A_2$) , where $\underline{d}_{e_g}$ stands for a $3d$ hole of e_g symmetry. The scattering causes $\underline{d}^2_{e_g} \rightarrow \underline{d}_{e_g}\underline{d}_{t_{2g}}$ transitions. In the absence of $1s$ spin-orbit coupling, spin is conserved. The final states that can be reached are of $^3T_1$ and $^3T_2$ symmetry. The $^3T_2$ is at 1 eV. The $\underline{d}_{e_g}\underline{d}_{t_{2g}}$ ($^3T_1$) configuration couples via the dd Coulomb interaction to the $\underline{d}^2_{t_{2g}}$ state of the same symmetry and leads to peaks 1.7 and 3 eV. A weak feature might also be visible around 0.5 eV, although it is hard to distinguish at this count rate due to the close proximity to the elastic line.

When increasing the excitation energy above the pre-edge feature, these local dd transitions are still visible. This is unexpected since quadrupolar features are very weak in the main absorption feature. Recently, dd features have also been observed in the $1s \rightarrow 4p$ region[7] in the quasi-zero-dimensional compound CuB_2O_4. Surprisingly, the strength in the pre-edge region of these excitations is rather small. Generally, excitations at the K-edge are shake-up excitations resulting from the transient presence of a strong core-hole potential in the intermediate state[4,13,14]. However, since the ground state contains only e_g holes, the involvement of t_{2g} electrons in the screening process is unlikely. In addition, the experiments are performed in a 90° scattering condition. This eliminates the possibility that the transitions are a result of the $\mathbf{A}^2$ term[15,16], which is zero in this geometry. Also, since the polarization vectors of the incoming and outgoing x-rays are perpendicular to each other, the orbital of the excited electron must have changed and the $4p$ electron can most likely not be considered a spectator. This change could be a result of hybridization between the $3d$ and $4p$ states on the site with the $1s$ core hole. This coupling is weak and for a quasi-zero-dimensional compound, such as CuB_2O_4, it is symmetry forbidden[7]. The coupling is present in three-dimensional systems, such as NiO and $NiCl_2$. However, it is difficult to understand why a hybridization mechanism would favor one particular $t_{2g}e_g$ multiplet over another. One would expect that a hybridization mechanism would give equal weight to the $^3T_2$ peak and the combined $^3T_1$ features. This is confirmed via numerical calculations based on a tight-binding model to estimate the $3d$-$4p$ mixing throughout the Brillouin zone (not shown). However, this contradicts with the experimental observations where the $^3T_2$ is significantly weaker, see Fig. 1. Here, we demonstrate that the dd features are due to Coulomb scattering of the excited $4p$ electron with the $3d$ states.

The relative strength of these excitations compared to the charge-transfer features at 4 eV and higher might at first seem surprising since the $3d$-$4p$ Coulomb interaction is significantly weaker than the $1s$-$3d$ interaction. In addition, the intensity of the transitions is approximately proportional to the square of the interaction strength. Charge-transfer excitations are excited by the interaction between the core-hole and valence shell, which is of the order of 6-8 eV. The dd excitations are due to higher-order terms in the $3d$-$4p$ Coulomb interaction which are of the order of tenths of an electron volt. This makes the excitation process about a factor 1000 smaller. Indeed these transitions are not visible in most scattering geometries. However, experimentally, a (typical) 90 degrees horizontal scattering condition is employed, which very strongly reduces the charge-transfer excitations since the incoming polarization vector is perpendicular to both outgoing polarization vectors. For a single NiO_6 cluster, the charge-transfer excitations are then forbidden. Within a crystal, these transitions become weakly allowed away from high-symmetry directions in the Brillouin zone. In addition, the resonant factor reduces the intensity by a factor $1/(E_f - E_g)^2$, where $E_f - E_g$ is the energy loss of the photon. This reduces the charge-transfer excitations by a factor 4-20 relative to the dd excitations. Therefore, due to the chosen scattering condition, the dd excitations are not negligibly weak compared to the charge-transfer excitations. The possible role of the $4p$ in the creation of

valence excitations has been indicated earlier[17]. In this following sections, we give a general treatment of the excitations due to 3*d*-4*p* Coulomb scattering.

III. THEORY

The RIXS cross section is well described by the Kramers-Heisenberg formula

$$I(\omega,\omega') \;=\; \sum_f |A(\omega,\mathbf{e}',\mathbf{e})|^2\delta(\hbar\omega' + E_f - \hbar\omega), \quad (1)$$

where

$$A(\omega,\mathbf{e}',\mathbf{e}) = \langle f|D'\frac{1}{\hbar\omega - H + i\Gamma}D|g\rangle \quad (2)$$

is the scattering amplitude where $|g\rangle$ and $|f\rangle$ are the ground and final states, respectively; $D \sim \mathbf{e}\cdot\mathbf{r}$ is the electric dipole operator with $\mathbf{e}$ the polarization vector; H is the Hamiltonian of the system and Γ the intermediate-state lifetime broadening. We take the ground-state energy $E_g = 0$. Although we also evaluate the cross section numerically using the above expression, a better understanding of the excitations created in the process is obtained by considering the relevant terms in the scattering amplitude. We are interested in the inelastic scattering terms arising from the indirect RIXS process[1] related to the 3*d*-4*p* Coulomb interaction contained in H'. For indirect RIXS, we can expand the scattering amplitude, which gives

$$A(\omega,\mathbf{e}',\mathbf{e}) = \langle f|D'\frac{1}{\hbar\omega - \hbar\omega' - H_0 + i\Gamma}H'\frac{1}{\hbar\omega - H + i\Gamma}D|g\rangle,$$

where $H_0 = H - H'$. We want to focus on excitation to lowest order, which necessitates some approximations. We can neglect all other intermediate state effects and treat the scattering to lowest-order. This leads to the result in lowest order perturbation

$$A(\omega,\mathbf{e}',\mathbf{e}) = \frac{1}{(\hbar\omega - \hbar\omega' - E_f + i\Gamma)(\hbar\omega + i\Gamma)}\langle f|D'H'D|g\rangle.$$

However, in general, intermediate-state interactions are not small and we need to treat the intermediate-state Hamiltonian with more care. An alternative approach to the scattering amplitude is the use of the ultra-short core-hole lifetime expansion[14]. Let us express the second Green's function in terms of $|n\rangle$ which are eigenstates of H_0,

$$\sum_{nn'}|n'\rangle\langle n'|\frac{1}{\hbar\omega - E_n - H' + i\Gamma}|n\rangle\langle n|D|g\rangle. \quad (3)$$

Generally, the intermediate-state lifetime broadening Γ is a large quantity, for example, of the order of a few eV for transition-metal K edges. Therefore, the fine structure due to H' is smaller than Γ. In this limit, we can neglect the effect of H' in the denominator and only consider the coupling in the numerator. This gives for the scattering amplitude

$$A(\omega,\mathbf{e}',\mathbf{e}) \;=\; \sum_n \frac{1}{(\hbar\omega - \hbar\omega' - E_f + i\Gamma)} \times\frac{1}{(\hbar\omega - E_n + i\Gamma)}\langle f|D'|n\rangle\langle n|H'|n\rangle\langle n|D|g\rangle.$$

The physical interpretation of this approximation at the transition-metal K edge is as follows. In the dipolar region transitions are made into the wide 4*p* band, creating intermediate states with an energy $E_n = E_{\underline{1s}} + E_{4p,n\mathbf{k}}$, where $E_{\underline{1s}}$ is the energy to create a deep-lying $\underline{1s}$ core hole and $E_{4p,n\mathbf{k}}$ is the energy of an electron in the 4*p* band with momentum $\mathbf{k}$ and band index n. The 4*p* band width is generally larger than the broadening Γ. However, the scattering between the intermediate states caused by H' is smaller than the broadening Γ. Since the effect of H' is already taken into account in the numerator, we neglect the higher-order effect in the denominator. In the emission process, the excited 4*p* electron decays and we are left with a *dd* excitation.

In both cases, the scattering amplitude can be split into $A(\omega,\mathbf{e}',\mathbf{e}) \cong \sum_n P_n(\omega,\omega')T_n(\mathbf{e}',\mathbf{e})$, where $P(\omega,\omega')$ is a scattering amplitude. The transitions are contained in $T_n(\mathbf{e}',\mathbf{e}) = \langle f|D|n\rangle\langle n|H'|n\rangle\langle n|D|g\rangle$ where the interaction H' is the term in the Hamiltonian responsible for creating the final state excitatons, which in our case is the Coulomb interaction between the excited 4*p* electron and the 3*d* shell. For an atom, H' can be written as[12,18]

$$H' = \sum_{\substack{kmm'qq'\\ \sigma_1\sigma_2\sigma_3\sigma_4}} \delta_{m'+q,m+q'}\left[c^k(dm,dm')c^k(pq',pq)F^k\delta_{\sigma_1\sigma_4}\delta_{\sigma_2\sigma_3} - c^k(pq',dm')c^k(dm,pq)G^k\delta_{\sigma_1\sigma_3}\delta_{\sigma_2\sigma_4}\right] p^\dagger_{q'\sigma_4}\underline{d}^\dagger_{m'\sigma_3}\underline{d}_{m\sigma_2}p_{q\sigma_1},$$

the angular moments are $p = 1$ and $d = 2$ (for clarity, symbols are used); $p^\dagger_{q\sigma}$ creates a 4*p* electron with orbital moment q and spin σ. For late transition-metal compounds, it is more convenient to look at the scattering of holes and $\underline{d}^\dagger_{m\sigma}$ creates a 3*d* hole with orbital moment m and spin σ. F^k and G^k are the radial matrix elements of the Coulomb interaction. The coefficients c^k arise from the integrations over the angular part of the wavefunction and are related to Clebsch-Gordan coefficients (3*j* symbols). In the Coulomb interaction for an atom, angular momentum is exchanged between the electrons. The first term on the right-hand side represents the direct scattering of a *p* and a *d* electron from angular momentum q and m' to q' and m, respectively (or from m to m' for the *d* hole). The second term is the exchange interaction, where the *p* and *d* electron are interchanged. At the K-edge, the angular momentum of the 4*p* electron is directly related to the polarization of the X-rays via the dipole operator $D \sim \sum_{q\sigma} e_q p^\dagger_{q\sigma}s_\sigma$ where s_σ creates a hole in the $1s$ core level. The components e_q of the unit polarization vector $\mathbf{e}$ can be expressed in (normalized) spherical harmonics in the direction of the polarization

vector $e_q = C_{1q}(\mathbf{e}) = \sqrt{4\pi/3}Y_{1q}(\mathbf{e})$. Due to the small Coulomb exchange interaction of the $1s$ core hole with the valence shell, the $1s$ spin is unlikely to change in the intermediate state. This also implies that the spin of the $4p$ electron cannot change in the scattering process, otherwise the dipole transition for the emission is no longer allowed. For our physical understanding, it is convenient to separate the scattering of the d and the p electrons. The exchange term of the p-d Coulomb can be recoupled[20] making it appear as a direct Coulomb interaction, giving for the transition operator

$$\begin{aligned} T_n &= \sum_{k=0}^{2}\sum_{mm'qq'\sigma}(2F^k - \sum_{k'=1,3} b_{kk'}G^{k'})\delta_{m'-m,q'-q} \\ &\times c^k(1q',1q)d_{n,qq'}C_{1q'}(\mathbf{e}')C_{1q}(\mathbf{e})c^k(dm,dm')\underline{d}^\dagger_{m'\sigma}\underline{d}_{m\sigma}, \end{aligned} \tag{4}$$

with the coefficient

$$b_{kk'} = \frac{(2k+1)n^2_{pk'd}}{n_{pkp}n_{dkd}} \left\{ \begin{array}{ccc} p & k' & p \\ d & k & d \end{array} \right\}, \tag{5}$$

where the bracketed term is a $6j$ symbol and the normalization constant

$$n_{xyz} \equiv \left(\begin{array}{ccc} x & y & z \\ 0 & 0 & 0 \end{array} \right) \tag{6}$$

is expressed as a $3j$ symbol. Since the ground and final states do not contain $4p$ electrons and $1s$ holes, the related operators can be removed from the expression in Eq. (4). The factor two in front of F^k derives from the fact that the spin of the excited $4p$ electron is irrelevant for direct scattering, whereas for the exchange term the spins of the scattered d and p electrons have to be equal. The effects of the $4p$ band are given in $d_{n,qq'} = |\langle n|p^\dagger_{q\sigma}|g\rangle|^2$, which is essentially the absorption strength for a particular $4p$ orbital. Let us now assume that $d_{n,qq'} = d_n$, i.e. the only polarization dependence comes from the polarization vectors and not from the details in the bandstructure. This condition is often well satisfied in the broad $4p$ bands. We then arrive at the central result for the effective transition operator

$$T_n(\mathbf{e}',\mathbf{e}) = \sum_{k=0}^{2}\sum_{\kappa=-k}^{k} d_n A_k \bar{U}^k_\kappa(\mathbf{e}',\mathbf{e})W^k_\kappa, \tag{7}$$

that consist of three distinct factors. The strength of the coupling

$$A_k = (2F^k - b_{k1}G^1 - b_{k3}G^3)n_{pk}n_{dk}, \tag{8}$$

with

$$n_{lx} \equiv \left(\begin{array}{ccc} l & x & l \\ -l & 0 & l \end{array} \right), \tag{9}$$

can be expressed in terms of the radial matrix elements of the pd Coulomb interaction as

$$A_0 = 2F^0 - \frac{2}{15}G^1 - \frac{3}{35}G^3 \tag{10}$$

$$A_1 = \frac{1}{5}G^1 + \frac{3}{35}G^3 \tag{11}$$

$$A_2 = \frac{4}{35}F^2 - \frac{1}{15}G^1 - \frac{3}{245}G^3. \tag{12}$$

The scattering in the valence shell is given in spherical coordinates in terms of a $3j$ symbol[20]

$$w^k_q = \sum_{mm'q} w^k_{mm'q}\underline{d}^\dagger_{m'\sigma}\underline{d}_{m\sigma}, \tag{13}$$

where k is the rank of the scattering operator with $q = k, k-1, \cdots, -k$ are the components. The coefficients are given by

$$w^k_{mm'q} = (-1)^{d-m'} \left(\begin{array}{ccc} d & k & d \\ -m' & q & m \end{array} \right) n^{-1}_{dk} \tag{14}$$

The coefficients $w^k_{mm'\sigma}$ form a 5×5 matrix $\mathrm{w}^k_{mm'\sigma}$. When considering $3d$ electrons, it is more convenient to deal with real orbitals. We can perform a unitary transformation[21,22]

$$W^k_\kappa = \sum_{q\mu\mu'\sigma} W^k_{\mu\mu'\kappa}\underline{d}^\dagger_{\mu'\sigma}\underline{d}_{\mu\sigma}, \tag{15}$$

where $W^k_{\mu\mu'\kappa}$ are the coefficients of the matrix

$$\mathrm{W}^k_\kappa = i^k \sum_q (\mathrm{Z}^k_{\kappa q})^\dagger (\mathrm{Z}^2)^\dagger w^k_q \mathrm{Z}^2, \tag{16}$$

where

$$\mathrm{Z}^2 = \left(\begin{array}{ccccc} \frac{1}{\sqrt{2}} & 0 & 0 & 0 & -\frac{i}{\sqrt{2}} \\ 0 & -\frac{1}{\sqrt{2}} & 0 & \frac{i}{\sqrt{2}} & 0 \\ 0 & 0 & 1 & 0 & 0 \\ 0 & \frac{1}{\sqrt{2}} & 0 & \frac{i}{\sqrt{2}} & 0 \\ \frac{1}{\sqrt{2}} & 0 & 0 & 0 & \frac{i}{\sqrt{2}} \end{array} \right) \begin{array}{c} |2\rangle \\ |1\rangle \\ |0\rangle \\ |-1\rangle \\ |-2\rangle \end{array}, \tag{17}$$

is a unitary transformation from atomic to tesseral (real) orbitals; note that $\kappa = 2, 1, 0, -1, -2 = x^2-y^2, zx, 3z^2-r^2, yz, zx$. Each of the operators has a particular angular dependence $\bar{U}^k_\kappa = \mathrm{sgn}(\kappa)U^k_\kappa$ given by the normalized tensor product $U^k_\kappa = [\mathbf{e}'^*, \mathbf{e}]^k_\kappa$ with

$$U^0_0(\mathbf{e}',\mathbf{e}) = \mathbf{e}'^* \cdot \mathbf{e} \tag{18}$$

and

$$U^1_\kappa(\mathbf{e}',\mathbf{e}) = (\mathbf{e}'^* \times \mathbf{e})_\kappa \tag{19}$$

with $\kappa = 1, 0, -1 = x, z, y$, and

$$U^2_2(\mathbf{e}',\mathbf{e}) = \sqrt{3}(e'^*_x e_x - e'^*_y e_y) \tag{20}$$

$$U^2_1(\mathbf{e}',\mathbf{e}) = \sqrt{3}(e'^*_z e_x + e'^*_x e_z) \tag{21}$$

$$U^2_0(\mathbf{e}',\mathbf{e}) = 2e'^*_z e_z - e'^*_x e_x - e'^*_y e_y \tag{22}$$

$$U^2_{-1}(\mathbf{e}',\mathbf{e}) = \sqrt{3}(e'^*_y e_z + e'^*_z e_y) \tag{23}$$

$$U^2_{-2}(\mathbf{e}',\mathbf{e}) = \sqrt{3}(e'^*_x e_y + e'^*_y e_x). \tag{24}$$

There is a remarkable similarity between the effective transition operator in Eq. (7) and those in RIXS at the transition-metal L- or M-edges[19]. Within the fast-collision approximation, the RIXS scattering operator at a particular edge can be expressed in terms of spin dependent and independent operators. The latter are, apart from a constant factor, given by T in Eq. (7), but with $d_n A_k \equiv 1$. The spin-dependent operators are due to the presence of the core-hole spin-orbit coupling and are not present for the scattering due to the $4p$-$3d$ Coulomb interaction.

IV. dd-TRANSITIONS IN NIO AND $NICL_2$

The simplest transition operator is due to the monopole part of the pd Coulomb interaction given by $k = 0$ and related to the F^0 radial matrix element. The effective operator is the number of holes $W_0^0 = n_h$. Since the symmetry does not change, it will not produce local dd excitations in NiO. However, it can give rise to charge-transfer type excitations of the same symmetry, although these are significantly smaller than the charge-transfer excitations due to the $1s$ core hole. For $k = 0$, the polarization part in Eq. (4) is given by the inner product $\bar{U}_\kappa^k(\mathbf{e}', \mathbf{e}) = \mathbf{e}'^* \cdot \mathbf{e}$. In a typical 90° horizontal scattering condition, this term is always zero, and we effectively "switch off" the monopole part of the pd Coulomb interaction.

Of more interest are local dd transitions resulting from angular momentum exchange between the $4p$ electron and the $3d$ valence band. For NiO, the ground state is $|^3A_2\rangle = |\underline{d}_{x^2-y^2\uparrow}\underline{d}_{3z^2-r^2\uparrow}\rangle$. This state $|^3A_2\rangle = |2\uparrow 0\uparrow\rangle$ in terms of tesseral harmonics. The operators W_κ^k directly couple the ground state to final state multiplets via $\underline{d}_{e_g} \rightarrow \underline{d}_{t_{2g}}$ transitions. For example, by evaluating the coefficients of the matrix in Eq. (15), we find, leaving out the spin part,

$$W_1^1|20\rangle = -\frac{1}{2}|0,-1\rangle + \frac{\sqrt{3}}{2}|2,-1\rangle \quad (25)$$

$$W_0^1|20\rangle = |0,-2\rangle \quad (26)$$

$$W_{-1}^1|20\rangle = -\frac{1}{2}|01\rangle - \frac{\sqrt{3}}{2}|21\rangle, \quad (27)$$

taking care of the commutation of the electrons. The quantum numbers are ordered such that the e_g holes ($\mu = 2, 0 = x^2-y^2, 3z^2-r^2$) are in front of the t_{2g} holes ($\mu = 1, -1, -2 = zx, yz, xy$). The symmetry of this state is not directly obvious. We can however rewrite

$$-\frac{1}{2}|0\rangle + \frac{\sqrt{3}}{2}|2\rangle = |3x^2-r^2\rangle \quad (28)$$

$$-\frac{1}{2}|0\rangle + \frac{\sqrt{3}}{2}|2\rangle = |3y^2-r^2\rangle \quad (29)$$

We can therefore also write the transitions as

$$W_1^1|20\rangle = |3x^2-r^2; yz\rangle = |T_2-1\rangle \quad (30)$$

$$W_0^1|20\rangle = |3z^2-r^2; xy\rangle = |T_2-2\rangle \quad (31)$$

$$W_{-1}^1|20\rangle = |3y^2-r^2; zx\rangle = |T_2 1\rangle. \quad (32)$$

The $3r_i^2 - r^2$ with $r_i = x, y, z$ orbitals are invariant under symmetry operations of the octahedral group. Therefore, the symmetry of the product wavefunctions is equivalent to that of the t_{2g} orbitals and the total symmetry is therefore T_2. Performing the same analysis for the transitions from W_κ^2, we can write

$$|^3T_2\kappa\rangle = W_\kappa^1|^3A_2\rangle \quad \text{for } \kappa = -2, -1, 1 \quad (33)$$

$$|^3T_1\kappa\rangle = W_\kappa^2|^3A_2\rangle \quad \text{for } \kappa = -1, 0, 1. \quad (34)$$

W_κ^1 and W_κ^2 also lead to $\underline{d}_{e_g} \rightarrow \underline{d}_{e_g}$ transitions, which are small due to spin conservation, and $\underline{d}_{t_{2g}} \rightarrow \underline{d}_{t_{2g}}$ transitions that can be neglected due to the small t_{2g} hole density in the ground state, respectively. Figure 2(a) gives a numerical calculation of the dd transitions for a NiO_6 cluster[16] where the $3d$-$4p$ Coulomb interaction has been included explicitly. The F^2 Coulomb term is directly related to the W^2 operator and results predominantly in $^3T_1$ spectal weight, see Fig. 2(a). Some small spectral weight is present in the $^3T_1$ due to higher-order effects and other intermediate state interactions. As a result of the recoupling, the G^1 term in the Coulomb interaction connects to the transition operators for $k = 0, 1, 2$. However, as can be seen from the coefficients A_k, the dominant scattering is related to the $k = 1$ term. For the $^3T_1$, the transition intensity due to G^1 is weaker relative to the F^2 by a factor $(12F^2/7G^1)^2 \cong 5$, for a typical ratio $G^1/F^2 = 0.75$. The scattering due to the G^3 term is small. The total spectrum in Fig. 2(a) reproduces the relatively weak spectral weight of the $^3T_2$ feature with respect to the $^3T_1$ peaks. Since the $4p$-$3d$ Coulomb interaction is relatively weak, these dd can generally not be easily distinguished from the much stronger charge-transfer excitations due to the $1s$ core hole. However, in a horizontal 90 degrees scattering geometry, see the inset in Fig. 2, the latter excitations are strongly reduced. For a single NiO_6 unit, they would be symmetry forbidden. For a solid, these transitions become weakly allowed away from high-symmetry axis in the Brillouin zone.

Since each of the component of the transition operators W_κ^k goes to a different final state, the angular dependence is approximately given by $\sum_{i,\kappa}(\bar{U}_\kappa^k(\mathbf{e}_i', \mathbf{e}))^2$ where $i = 1, 2$ for the polarization vectors of the outgoing x-rays. For a horizontal 90 degrees scattering geometry, $\mathbf{U}^1 = \mathbf{e}_i'^* \times \mathbf{e} = -\mathbf{e}_2, -\mathbf{e}_1$ for $i = 1, 2$, respectively. The angular dependence is then simply the norm of the polarization vectors and therefore a constant, , see the inset in Fig. 2. For $k = 2$, the angular dependence is more complex, but straightforward to evaluate. The strongest intensity occurs when the incoming polarization vector is along a crystal axis, see Fig. 2.

V. CONCLUSIONS

We have demonstrated experimentally the existence of *dd* excitations in RIXS in the $1s \rightarrow 4p$ region in NiO and $NiCl_2$. The origin of these features is an indirect RIXS process[14] involving the Coulomb interaction between the excited $4p$ electron and the $3d$ valence electrons creating a local *dd* multiplet and while changing the properties of the $4p$ electron. By employing a polarization condition that is sensitive to the changes in the $4p$ electron, *dd* excitations can be selectively probed. The observation of *dd* excitations with hard X-rays provides unique benefits for applications in complex materials under real conditions[23]. At the transition-metal K edges, *dd* excitations can often be observed in the pre-edge region. This is a direct RIXS process, which is more straightforward to interpret[5]. The relative intensities of the direct and indirect RIXS processes is difficult to determine and requires more experimental and theoretical investigation.

VI. ACKNOWLEDGEMENTS.

We acknowledge Yuri Shvyd'ko and Mary Upton for experimental support and discussions with George Sawatzky and Jeroen van den Brink. MvV was supported by the U.S. Department of Energy (DOE), Office of Basic Energy Sciences, Division of Materials Sciences and Engineering under contract DE-FG02-03ER46097 and the RIXS collaboration as part of the Computational Materials Science Network (CMSN) under grant DE-FG02-08ER46540. The experimental work was supported by DOE OBER & NIH EB001962. Work at Argonne National Laboratory was supported by the U.S. DOE, Office of Science, Office of Basic Energy Sciences, under contract DE-AC02-06CH11357.

[1] For a review, see L. J. P Ament, M. van Veenendaal, T. P. Devereaux, J. P. Hill, and J. van den Brink, arXiv:1009.3630.
[2] S. G. Chiuzbăian, G. Ghiringhelli, C. Dallera, M. Grioni, P. Amann, X. Wang, and L. Braicovich, Phys. Rev. Lett. **95**, 197402 (2005)
[3] G. Ghiringhelli, A. Piazzalunga, C. Dallera, T. Schmitt, V. N. Strocov, J. Schlappa, L. Patthey, X. Wang, H. Berger, and M. Grioni, Phys. Rev. Lett. **102**, 027401 (2009).
[4] J. P. Hill, C.C. Kao, W. A. L. Caliebe, M. Matsubara, A. Kotani, J. L. Peng, and R. L. Greene, Phys. Rev. Lett. **80**, 4967 (1998).
[5] S. Huotari, T. Pylkk¨anen, G. Vankó, R. Verbeni, and G. Monaco, Phys. Rev. B **78**, 041102 (2008).
[6] J. P. Hill, G. Blumberg, Y.-J. Kim, D. S. Ellis, S. Wakimoto, R. J. Birgenau, S. Komiya, Y. Ando, B. Liang, R. L. Greene, D. Casa, and T. Gog, Phys. Rev. Lett. **100**, 097001 (2008).
[7] J. N. Hancock, G. Chabot-Couture, Y. Li, G. A. Petrakovskii, K. Ishii, I. Jarrige, J. Mizuki, T. P. Devereaux, and M. Greven, Phys. Rev. B **80**, 092509 (2009).
[8] J. C. Fontecilla-Camps, P. Amara, C. Cavazza Y. Nicolet, and A. Volbeda, Nature **460**, 814 (2009).
[9] M.-E. Pandelia, H. Ogata, W. Lubitz, Chem. Phys. Chem. **11**, 1127 (2010).
[10] S.-l. Chen, V. Pelmenschikov, M. R. A. Blomberg, P. E. M. Siegbahn, J. Am. Chem. Soc. **131**, 9912 (2009).
[11] S. W. Ragsdale, Crit. Rev. Biochem. Mol. Biol. **39**, 165 (2004).
[12] J. S. Griffith, *The Theory of Transition-Metal Ions* (Cambridge University Press, Cambridge, 1961).
[13] M. A. van Veenendaal and G. A. Sawatzky, Phys. Rev. Lett. **70**, 2459 (1993).
[14] J. van den Brink and M. van Veenendaal, Europhys. Lett. **73**, 121 (2006).
[15] B. C. Larson, W. Ku, J. Z. Tischler, C.-C. Lee, O. D. Restrepo, A. G. Eguiluz, P. Zschack, and K. D. Finkelstein, Phys. Rev. Lett. **99**, 026401 (2007).
[16] M. W. Haverkort, A. Tanaka, L. H. Tjeng, and G. A. Sawatzky, Phys. Rev. Lett. **99**, 257401 (2007).
[17] H. Kondo, S. Ishihara, and S. Maekawa, Phys. Rev. B **64**, 014414 (2001); T. Inami, T. Fukuda, J. Mizuki, S. Ishihara, H. Kondo, H. Nakao, T. Matsamura, K. Hirota, Y. Murakami, S. Maekawa, and Y. Endoh, *ibid.* **67**, 045108 (2003);
[18] R. D. Cowan, it The Theory of Atomic Structure and Spectra (University of California Press, Berkeley, 1981).
[19] M. van Veenendaal, Phys. Rev. Lett. **96**, 117404 (2006).
[20] B. T. Thole, G. van der Laan, and M. Fabrizio, Phys. Rev. B **50**, 11 466 (1994); B. T. Thole and G. van der Laan, *ibid.* **50**, 11 474 (1994).
[21] M. van Veenendaal and M. W. Haverkort, Phys. Rev. B **77**, 224107 (2008).
[22] M. van Veenendaal, unpublished.
[23] X. Liu, M. Carpenter, Y. Shvydko, M. Upton, M. van Veenendaal, D. J. Bungum, G. Hillhouse, and S. P. Cramer, unpublished.

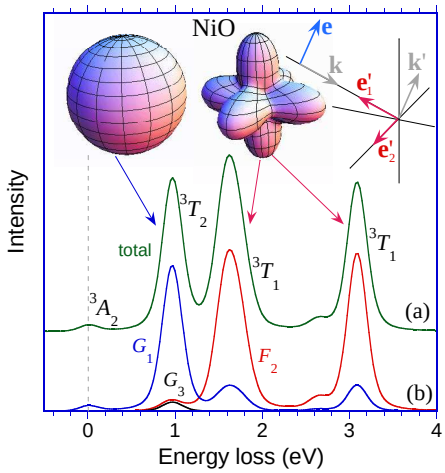

FIG. 2: (color online) (a) The total RIXS intensity due to the *pd* Coulomb interaction between the excited $4p$ electron and the $3d$ valence electrons in the intermediate state. A 90° horizontal scattering condition with the incoming polarization vectors 45° with respect to the z axis is used, see inset. (b) The RIXS intensity but now separated into different terms in the *pd* Coulomb interaction, where F^2 is related to the direct interaction and G^1 and G^3 are exchange interactions. The top shows the angular distributions as a function of the direction of the incoming polarization vector.